Supplementary material for: Equilibrium-nonequilibrium ring-polymer molecular dynamics for nonlinear spectroscopy

Tomislav Begušić,[1, a)] Xuecheng Tao,[1] Geoffrey A. Blake,[1, 2] and Thomas F. Miller III[1]

[1)] *Division of Chemistry and Chemical Engineering, California Institute of Technology, Pasadena, California 91125, USA*

[2)] *Division of Geological and Planetary Sciences, California Institute of Technology, Pasadena, California 91125, USA*

(Dated: 13 March 2022)

[a)] Electronic mail: tbegusic@caltech.edu

I. COMPUTATIONAL DETAILS

A. One-dimensional model

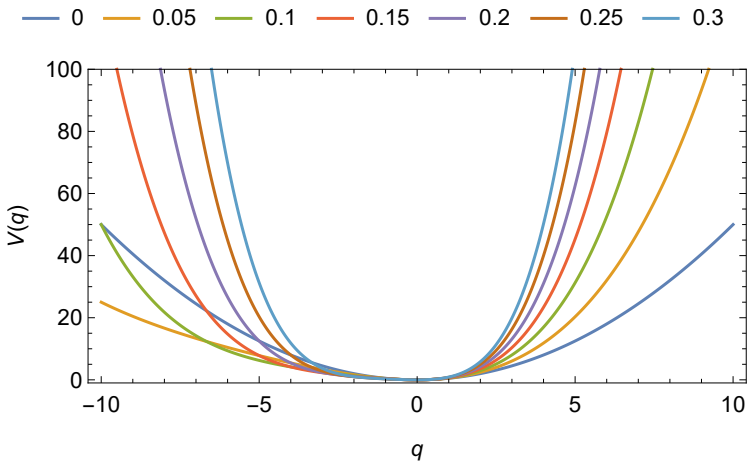

FIG. 1. Potentials $V(q) = 0.5q^2 + aq^3 + a^2q^4$ of varying degree of anharmonicity, controlled by the parameter a, plotted on the position grid used in quantum calculations.

Here, the response function $R(t_2, t_1)$ was computed for 120 steps along both time coordinates with a time step of 0.25, with the exact result obtained by solving the time-independent Schrödinger equation on a position grid (see Fig. 1) ranging from -10 to 10 with a step of 0.01 and transforming the operators $\hat{A}$, $\hat{B}$, and $\hat{C}$ to the eigenstate basis. Depending on the temperature, between 10 and 60 states were used in the evaluation of the response function. The same approach was used for computing the exact DKT correlation function. Since the relation between the DKT correlation function $K(t_2, t_1)$ and $R(t_2, t_1)$ assumes a Fourier transform involving both positive and negative t_1 and t_2, DKT correlation functions were computed for positive and negative times, i.e., from -30 to 30. In addition, the Fourier transform assumes infinite integral boundaries, which can be replaced by final times only if the integrand is zero beyond some time. This is usually the case because correlation functions are typically damped by the environment. In our simple system, no damping is applied to the correlation functions, which is why the relation between the computed $K(t_2, t_1)$ and $R(t_2, t_1)$ holds only approximately. To avoid artifacts due to boundary effects, the Fourier transform of the DKT correlation function, $K(\omega_2, \omega_1)$, was multiplied by $\exp[-0.02(\omega_1^2 + \omega_2^2)]$. For the same reason, only $t_1, t_2 < 27.5$ are used to offer a fair comparison between DKT-based and

other methods. Figure 2 shows that the numerical error introduced in this way is negligible.

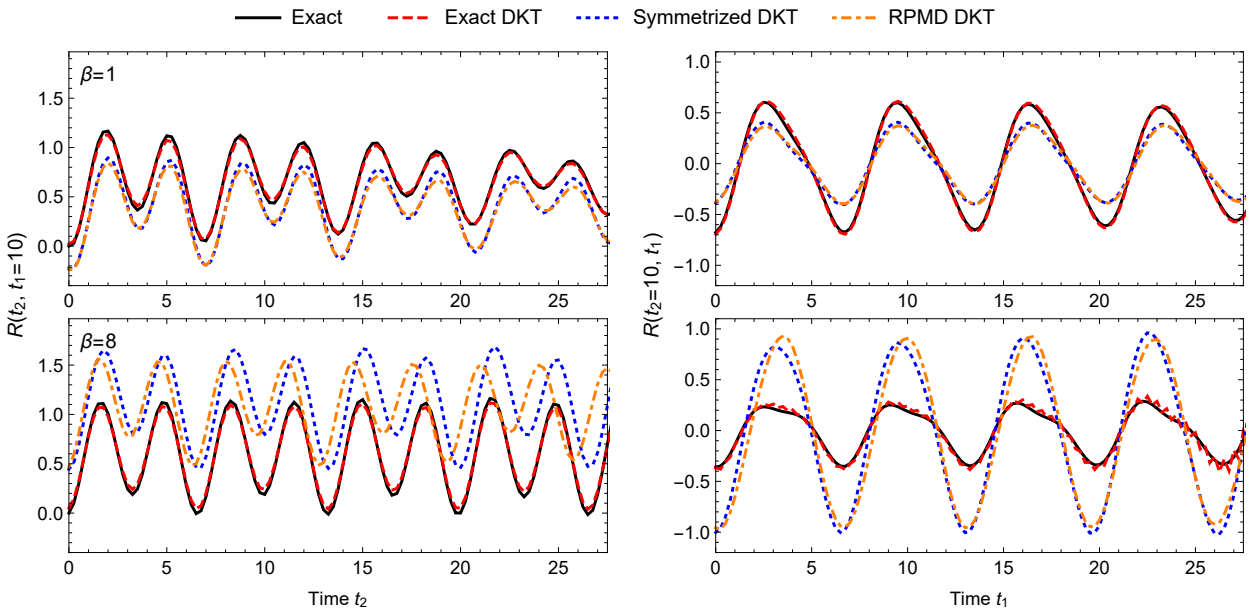

FIG. 2. Same as Fig. 2 of the main text, but comparing two exact quantum simulations of the response function, using either the direct evaluation or the DKT correlation function, and two approximate calculations based on the symmetrized DKT correlation function and its RPMD approximation.

To obtain classical and RPMD results, $K = 2^{17} \approx 10^5$ initial conditions $(q^{(k)}, p^{(k)})$ were sampled from a thermal trajectory computed using the Andersen thermostat.[1] Then, four trajectories were run for each initial condition: two nonequilibrium trajectories starting from $(q^{(k)}, p^{(k)} \pm (\varepsilon_2/2) N[\partial B_N(q^{(k)})/\partial q^{(k)}])$ with $\varepsilon = 0.01$ (see Fig. 3), a forward trajectory starting from $(q^{(k)}, p^{(k)})$, and a backward trajectory that is computed by propagating $(q^{(k)}, -p^{(k)})$ forward in time. Trajectories were propagated using a second-order symplectic algorithm[2] with a time step of 0.05 for 600 steps, while the observables were evaluated every 5 steps of the dynamics. Classical results were obtained by setting the number of beads $N = 1$, while $N = 64$ was used for the converged RPMD results. The nonequilibrium and backward trajectories were used for evaluating the equilibrium-nonequilibrium response function according to

$$R(t_2, t_1) = -\frac{\partial}{\partial t_1} \left\{ \frac{\beta}{K\varepsilon_2} \sum_{k=1}^{K} [C_N(q^{(k)}_{+,t_2}) - C_N(q^{(k)}_{-,t_2})] A_N(q^{(k)}_{-t_1}) \right\}, \tag{1}$$

where the time derivative was computed numerically. The forward and backward equilibrium trajectories were used for evaluating the RPMD DKT response function for positive and

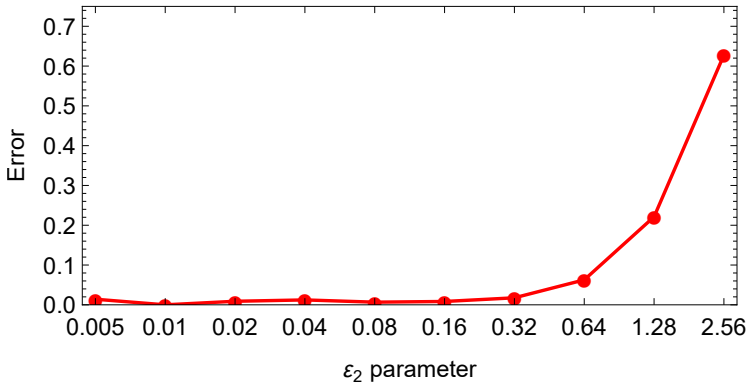

FIG. 3. Effect of the ε_2 parameter on the equilibrium-nonequilibrium RPMD response function. Error is measured by Eq. (38) of the main text with $R^{\text{exact}}(t_2, t_1)$ replaced by the RPMD response function computed with $\varepsilon_2 = 0.01$. Figure shows that the results are not affected by the choice of ε_2 for a wide range of values.

negative t_1 and t_2 times.

B. Two-dimensional model

The two-time response function of the two-dimensional model was evaluated for 200 steps (time step 0.25) in t_1 and t_2. Exact results were obtained in the same way as for the one-dimensional system, using a two-dimensional grid between -20 and 20 (step 0.01) along each coordinate and the first 50 eigenstates. For the RPMD ($N = 64$) and classical ($N = 1$) simulations, we averaged the response function over 2^{17} samples and the trajectories were run for 1000 steps (time step 0.05, observables evaluated every 5 steps). External field parameter was $\varepsilon_2 = 0.01$.

Spectra for the two-dimensional model were evaluated as

$$S_C(\omega_2, \omega_1) = \int_0^\infty dt_2 \int_0^\infty dt_1 R(t_2, t_1) e^{-(t_1+t_2)/\tau} \cos(\omega_1 t_1) \cos(\omega_2 t_2), \tag{2}$$

where $\tau = 7.5$. Before taking the discrete cosine transform, the damped response function was padded with zeros up to $t_1, t_2 = 1300$. The double cosine transform of Eq. (2) is related to the Fourier transform

$$S_F(\omega_2, \omega_1) = \int_0^\infty dt_2 \int_0^\infty dt_1 R(t_2, t_1) e^{-(t_1+t_2)/\tau} e^{-i\omega_1 t_1 - i\omega_2 t_2} \tag{3}$$

by

$$S(\omega_2, \omega_1) = \frac{1}{2}\mathrm{Re}[S_F(\omega_2, \omega_1) + S_F(-\omega_2, \omega_1)]. \tag{4}$$

An alternative is to use the sine transform

$$S_S(\omega_2, \omega_1) = \int_0^\infty dt_2 \int_0^\infty dt_1 R(t_2, t_1) e^{-(t_1+t_2)/\tau} \sin(\omega_1 t_1) \sin(\omega_2 t_2) \tag{5}$$

$$= -\frac{1}{2}\mathrm{Re}[S_F(\omega_2, \omega_1) - S_F(-\omega_2, \omega_1)], \tag{6}$$

which was proposed in Ref. 3 as a way to extract the purely absorptive component of the two-dimensional spectrum. We show these different transforms in Fig. 4. In this case, the main off-diagonal peak at $(\omega_1, \omega_2) \approx (\Omega_1 = 0.5, \Omega_2 = 2.0)$ does not appear in the sine transform, but is well resolved in the cosine transform. The peaks appearing in the Fourier transform spectrum (Fig. 4, middle) can be assigned to the Feynman diagrams of Ref. 4.

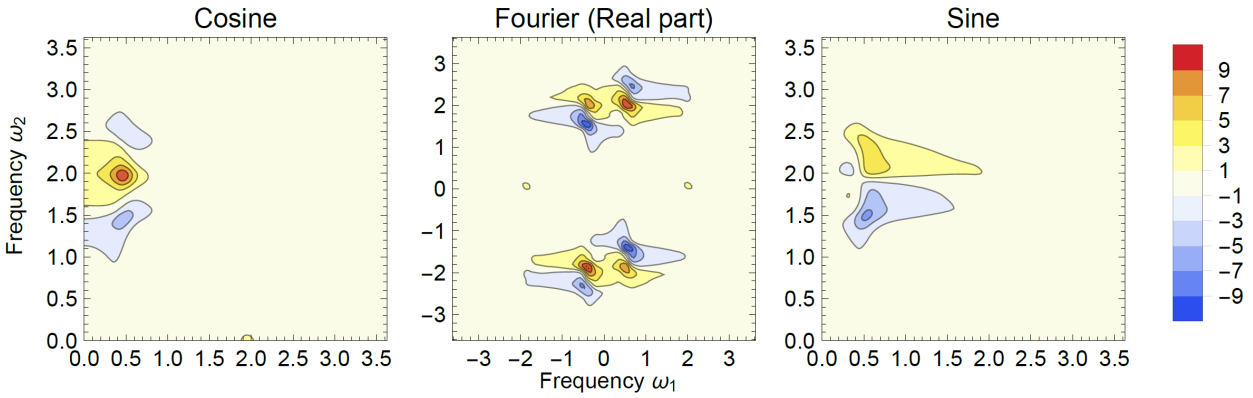

FIG. 4. Cosine [Eq. (2)], Fourier [Eq. (3), real part], and sine [Eq. (5)] transforms of the damped two-time response function of the two-mode system, presented in the main text, evaluated with exact quantum dynamics at $\beta = 8$.

II. HARMONIC LIMIT

In this Section, we show that the RPMD method proposed in the main text is exact in the limit $N \to \infty$ for the harmonic oscillator,

$$V(q) = \frac{1}{2}m\omega^2 q^2, \tag{7}$$

and when two of the operators $\hat{A}$, $\hat{B}$, and $\hat{C}$ are linear in position.

A. Quantum response functions

To derive the exact quantum results, we first rewrite

$$R(t_2,t_1) = -\frac{1}{\hbar^2}\mathrm{Tr}\left\{\hat{C}(t_2+t_1)[\hat{B}(t_1),[\hat{A},\hat{\rho}]]\right\} \tag{8}$$

$$= -\frac{1}{\hbar^2}\mathrm{Tr}\left\{[[\hat{C}(t_2+t_1),\hat{B}(t_1)],\hat{A}]\hat{\rho}\right\} \tag{9}$$

$$= -\frac{1}{\hbar^2}\left\langle[[\hat{C}(t_2+t_1),\hat{B}(t_1)],\hat{A}]\right\rangle \tag{10}$$

and note that

$$[\hat{q}(t),f(\hat{q})] = \frac{1}{m\omega}[\hat{p},f(\hat{q})] = -\frac{i\hbar}{m\omega}f'(\hat{q})\sin\omega t, \tag{11}$$

where $f'(q) = \partial f/\partial q$.

Then, for $\hat{A} = \hat{B} = \hat{q}$ and $\hat{C} = C(\hat{q})$, we have

$$R(t_2,t_1) = -\frac{1}{\hbar^2}\left\langle[[C(\hat{q}),\hat{q}(-t_2)],\hat{q}(-t_1-t_2)]\right\rangle \tag{12}$$

$$= -\frac{1}{\hbar^2}\left(-\frac{i\hbar}{m\omega}\right)\sin\omega t_2\left\langle[C'(\hat{q}),\hat{q}(-t_1-t_2)]\right\rangle \tag{13}$$

$$= \frac{i}{m\hbar\omega}\sin\omega t_2\left(-\frac{i\hbar}{m\omega}\right)\sin\omega(t_1+t_2)\left\langle C''(\hat{q})\right\rangle \tag{14}$$

$$= \frac{\langle C''(\hat{q})\rangle}{(m\omega)^2}\sin\omega t_2\sin\omega(t_1+t_2), \tag{15}$$

where we applied Eq. (11) twice. For $\hat{A} = \hat{C} = \hat{q}$ and $\hat{B} = B(\hat{q})$:

$$R(t_2,t_1) = -\frac{1}{\hbar^2}\left\langle[[\hat{q}(t_2),B(\hat{q})],\hat{q}(-t_1)]\right\rangle \tag{16}$$

$$= -\frac{1}{\hbar^2}\left(-\frac{i\hbar}{m\omega}\right)\sin\omega t_2\left\langle[B'(\hat{q}),\hat{q}(-t_1)]\right\rangle \tag{17}$$

$$= \frac{\langle B''(\hat{q})\rangle}{(m\omega)^2}\sin\omega t_1\sin\omega t_2. \tag{18}$$

For $\hat{B} = \hat{C} = \hat{q}$ and $\hat{A} = A(\hat{q})$:

$$R(t_2,t_1) = -\frac{1}{\hbar^2}\left\langle[[\hat{q}(t_2),\hat{q}],\hat{A}(-t_1)]\right\rangle \tag{19}$$

$$= -\frac{1}{\hbar^2}\left\langle\left[\left(-\frac{i\hbar}{m\omega}\right)\sin\omega t_2,\hat{A}(-t_1)\right]\right\rangle \tag{20}$$

$$= 0, \tag{21}$$

because scalars commute with operators.

B. RPMD response functions

Assuming ε_2 is small, we can derive the fully equilibrium RPMD from the equilibrium-nonequilibrium RPMD:

$$R(t_2,t_1) = \frac{\beta}{\varepsilon_2}\langle[C_N(q_{+,t_2}) - C_N(q_{-,t_2})]\dot{A}_N(q_{-t_1})\rangle, \tag{22}$$

$$= N\beta\left\langle\left[\frac{\partial C_N(q_{t_2})}{\partial q_{t_2}}\right]^T \cdot M_{qp,t_2}\cdot\frac{\partial B_N(q)}{\partial q}\dot{A}_N(q_{-t_1})\right\rangle, \tag{23}$$

where we used

$$C_N(q_{\pm,t_2}) \approx C_N(q_{t_2}) \pm \frac{\varepsilon_2}{2}\left[\frac{\partial C_N(q_{t_2})}{\partial p}\right]^T \cdot N\frac{\partial B_N(q)}{\partial q} \tag{24}$$

$$\approx C_N(q_{t_2}) \pm \frac{\varepsilon_2}{2}N\left[\frac{\partial C_N(q_{t_2})}{\partial q_{t_2}}\right]^T \cdot \frac{\partial q_{t_2}}{\partial p}\cdot\frac{\partial B_N(q)}{\partial q} \tag{25}$$

and defined $M_{xy,t} = \partial x_t/\partial y$. Equation (23) provides yet another way to employ RPMD in the simulation of two-time response function $R(t_2,t_1)$. Similar to the hybrid equilibrium-nonequilibrium approach, the equilibrium method also reduces to its classical MD analogue.[5–7] However, this method is less practical due to the need for computing and converging the stability matrix element M_{qp,t_2}, which has been deemed difficult even in the classical MD setting. Finally, we note that the equilibrium-nonequilibrium and fully equilibrium methods give equal results when ε_2 is small.

Before continuing with specific cases, we rewrite Eq. (23)

$$R(t_2,t_1) = N\beta\left\langle\left[\frac{\partial\tilde{C}_N(\tilde{q}_{t_2})}{\partial\tilde{q}_{t_2}}\right]^T \cdot M_{\tilde{q}\tilde{p},t_2}\cdot\frac{\partial\tilde{B}_N(\tilde{q})}{\partial\tilde{q}}\dot{\tilde{A}}_N(\tilde{q}_{-t_1})\right\rangle, \tag{26}$$

in terms of the ring-polymer normal mode coordinates $\tilde{q} = O\cdot q$, where O is an orthogonal $N\times N$ matrix that diagonalizes the ring-polymer force-constant and $\tilde{f}(\tilde{q}) = f(q)$. Specifically, the first normal mode $\tilde{q}_1 = \sqrt{N}q_c$ is a scalar multiple of the ring-polymer centroid $q_c = \frac{1}{N}\sum_{i=1}^N q_i$ and evolves according to

$$\tilde{q}_{1,t} = \tilde{q}_1\cos\omega t + \frac{1}{m\omega}\tilde{p}_1\sin\omega t. \tag{27}$$

Then, for $A(q) = B(q) = q$ and arbitrary $C(q)$, we have:

$$R(t_2,t_1) = N\beta \left\langle \frac{\partial \tilde{C}_N(\tilde{q}_{t_2})}{\partial \tilde{q}_{1,t_2}} M_{\tilde{q}_1\tilde{p}_1,t_2} \frac{1}{\sqrt{N}} \dot{\tilde{A}}_N(\tilde{q}_{-t_1}) \right\rangle \tag{28}$$

$$= \frac{\sqrt{N}\beta}{m\omega} \sin\omega t_2 \left\langle \frac{\partial \tilde{C}_N(\tilde{q}_{t_2})}{\partial \tilde{q}_{1,t_2}} \dot{\tilde{A}}_N(\tilde{q}_{-t_1}) \right\rangle \tag{29}$$

$$= \frac{\sqrt{N}\beta}{m\omega} \sin\omega t_2 \left\langle \frac{\partial \tilde{C}_N(\tilde{q})}{\partial \tilde{q}_1} \dot{\tilde{A}}_N(\tilde{q}_{-t_1-t_2}) \right\rangle \tag{30}$$

$$= \frac{\beta}{m} \sin\omega t_2 \sin\omega(t_1+t_2) \left\langle \frac{\partial \tilde{C}_N(\tilde{q})}{\partial \tilde{q}_1} \tilde{q}_1 \right\rangle \tag{31}$$

$$= \frac{N}{(m\omega)^2} \left\langle \frac{\partial^2 \tilde{C}_N(\tilde{q})}{\partial \tilde{q}_1^2} \right\rangle \sin\omega t_2 \sin\omega(t_1+t_2) \tag{32}$$

$$= \frac{1}{(m\omega)^2} \left\langle \frac{1}{N}\sum_{i=1}^{N} \frac{\partial^2 C(q_i)}{\partial q_i^2} \right\rangle \sin\omega t_2 \sin\omega(t_1+t_2), \tag{33}$$

$$= \frac{\langle C'' \rangle^{\mathrm{RP}}}{(m\omega)^2} \sin\omega t_2 \sin\omega(t_1+t_2), \tag{34}$$

where we used $\tilde{A}_N(\tilde{q}) = \tilde{B}_N(\tilde{q}) = q_c$, $\partial q_c/\partial \tilde{q}_1 = 1/\sqrt{N}$, and $\partial \tilde{q}_{i,t}/\partial \tilde{p}_1 = \delta_{i1} \sin\omega t/(m\omega)$ in Eqs. (28) and (29), $\dot{\tilde{A}}_N(\tilde{q}_t) = -(\omega/\sqrt{N})\tilde{q}_1 \sin\omega t + (1/m\sqrt{N})\tilde{p}_1 \cos\omega t$ to derive Eq. (31), in which we immediately dropped the second term that vanishes, because $\langle p_1 \rangle = 0$, and $\tilde{q}_1 \exp(-\beta_N H_N) = -(N/\beta m\omega^2)(\partial/\partial \tilde{q}_1) \exp(-\beta_N H_N)$ together with the integration by parts to obtain Eq. (32). Finally, Eq. (33) follows from Eq. (32) because

$$\frac{\partial^2 \tilde{C}_N(\tilde{q})}{\partial \tilde{q}_1^2} = \left(\frac{\partial q}{\partial \tilde{q}_1}\right)^T \cdot \frac{\partial^2 C_N(q)}{\partial q^2} \cdot \frac{\partial q}{\partial \tilde{q}_1} = \frac{1}{N} e^T \cdot \frac{\partial^2 C_N(q)}{\partial q^2} \cdot e = \frac{1}{N^2} \sum_{i=1}^{N} \frac{\partial^2 C(q_i)}{\partial q_i}, \tag{35}$$

where we used $\partial q/\partial \tilde{q}_1 = e/\sqrt{N}$ and defined the N-dimensional vector $e = (1 \ldots 1)^T$. In the limit of $N \to \infty$, Eq. (33) converges to the quantum result (15). Similarly, for $A(q) = C(q) = q$ and arbitrary $B(q)$:

$$R(t_2,t_1) = N\beta \left\langle \frac{1}{\sqrt{N}} \frac{1}{m\omega} \sin\omega t_2 \frac{\partial \tilde{B}_N(\tilde{q})}{\partial \tilde{q}_1} \frac{\omega}{\sqrt{N}} \tilde{q}_1 \sin\omega t_1 \right\rangle \tag{36}$$

$$= \frac{\beta}{m} \left\langle \frac{\partial \tilde{B}_N(\tilde{q})}{\partial \tilde{q}_1} \tilde{q}_1 \right\rangle \sin\omega t_1 \sin\omega t_2 \tag{37}$$

$$= \frac{\langle B'' \rangle^{\mathrm{RP}}}{(m\omega)^2} \sin\omega t_1 \sin\omega t_2, \tag{38}$$

which reduces to the corresponding quantum expression (18) when converged with respect

to the number of beads N. Finally, for $B(q) = C(q) = q$,

$$R(t_2, t_1) = N\beta \left\langle \frac{1}{\sqrt{N}} \frac{1}{m\omega} \sin \omega t_2 \frac{1}{\sqrt{N}} \dot{\tilde{A}}_N(\tilde{q}_{-t_1}) \right\rangle \tag{39}$$

$$= \frac{1}{m\omega} \sin \omega t_2 \left\langle \dot{\tilde{A}}_N(\tilde{q}_{-t_1}) \right\rangle = 0, \tag{40}$$

because equilibrium expectation values are time-independent.

Interestingly, in certain cases, even the classical method ($N = 1$) is exact. This is trivially true for the last studied case [$B(q) = C(q) = q$], but also for certain non-trivial cases, e.g., for $C(q) \propto q^2$ in the first studied example [$A(q) = B(q) = q$] and $B(q) \propto q^2$ in the second studied case [$A(q) = C(q) = q$] because the corresponding final expressions are independent of temperature. This can be seen in Fig. 3a of the main text for the anharmonicity parameter $a = 0$, $A(q) = B(q) = q$, and $C(q) = q^2/2$, where both classical and RPMD results are exact.

III. TWO-MODE SYSTEM IN THE ABSENCE OF COUPLING OR ANHARMONICITY

In the main text we showed spectra for the system described by the Hamiltonian $\hat{H}_{\mathrm{2D}}$ [see Eq. (37) of the main text] and operators $\hat{A} = \hat{q}_1$ and $\hat{B} = \hat{C} = \hat{q}_2$. The corresponding two-time response function

$$R(t_2, t_1) = -\frac{1}{\hbar^2} \mathrm{Tr} \left\{ \hat{q}_2(t_2 + t_1)[\hat{q}_2(t_1), [\hat{q}_1, \hat{\rho}]] \right\} \tag{41}$$

can be shown to vanish in the absence of coupling ($\lambda = 0$) or anharmonicity ($a = 0$). In the limit $\lambda = 0$, $\hat{\rho} = \hat{\rho}_1 \hat{\rho}_2$ and, therefore,

$$R(t_2, t_1) = -\frac{1}{\hbar^2} \mathrm{Tr}_{q_2} \left\{ \hat{q}_2(t_2 + t_1)[\hat{q}_2(t_1), \hat{\rho}_2] \right\} \mathrm{Tr}_{q_1} \left\{ [\hat{q}_1, \hat{\rho}_1] \right\} = 0, \tag{42}$$

because the trace of a commutator is zero. If $a = 0$, the system is harmonic, which means it can be decomposed into normal modes. Since all operators are linear in q_1 and q_2, they will also be linear in the normal-mode coordinates and, as shown in the previous Section, the response function is zero for linear operators in a harmonic potential.

REFERENCES

[1]H. C. Andersen, J. Chem. Phys. **72**, 2384 (1980).

[2]M. Ceriotti, M. Parrinello, T. E. Markland, and D. E. Manolopoulos, J. Chem. Phys. **133**, 124104 (2010).

[3]P. Hamm and J. Savolainen, J. Chem. Phys. **136**, 094516 (2012).

[4]L. Vietze, E. H. G. Backus, M. Bonn, and M. Grechko, J. Chem. Phys. **154**, 174201 (2021).

[5]S. Saito and I. Ohmine, Phys. Rev. Lett. **88**, 207401 (2002).

[6]S. Saito and I. Ohmine, J. Chem. Phys. **119**, 9073 (2003).

[7]T. Hasegawa and Y. Tanimura, J. Chem. Phys. **125**, 074512 (2006).